

Finite-size scaling of percolation on scale-free networks

Xuewei Zhao,¹ Liwenying Yang,¹ Dan Peng,² Run-Ran Liu,³ and Ming Li^{1,*}

¹*School of Physics, Hefei University of Technology, Hefei 230009, China*

²*School of Journalism and Communication, Anhui University, Hefei 230601, China*

³*Alibaba Research Center for Complexity Sciences, Hangzhou Normal University, Hangzhou 311121, China*

(Dated: July 9, 2025)

Critical phenomena on scale-free networks with a degree distribution $p_k \sim k^{-\lambda}$ exhibit rich finite-size effects due to its structural heterogeneity. We systematically study the finite-size scaling of percolation and identify two distinct crossover routes to mean-field behavior: one controlled by the degree exponent λ , the other by the degree cutoff $K \sim V^\kappa$, where V is the system size and $\kappa \in [0, 1]$ is the cutoff exponent. Increasing λ or decreasing κ suppresses heterogeneity and drives the system toward mean-field behavior, with logarithmic corrections near the marginal case. These findings provide a unified picture of the crossover from heterogeneous to homogeneous criticality. In the crossover regime, we observe rich finite-size phenomena, including the transition from vanishing to divergent susceptibility, distinct exponents for the shift and fluctuation of pseudocritical points, and a numerical clarification of previous theoretical debates.

I. INTRODUCTION

Due to the nontrivial topological features, network ensembles have emerged as a powerful platform for exploring the theories and methodologies of statistical physics [1]. Unlike lattice systems, which possess homogeneous and spatially embedded topologies, networks often lack spatial constraints. Instead, network ensembles are typically characterized by their degree distribution p_k [2–4], which gives the probability that a randomly selected node in the network has degree k , i.e., is connected to k other nodes.

A typical network ensemble is the Erdős-Rényi (ER) random graph [5], which follows a Poisson degree distribution. In the ER model, a fixed number E of links is randomly placed among V nodes, or alternatively, each pair of nodes is connected with a fixed probability. Owing to the absence of spatial constraints and the homogeneity of the degree distribution, critical phenomena in ER random graphs exhibit standard mean-field behavior [1]. In contrast, scale-free (SF) networks, which serve as a key organizing principle in many real-world systems [6, 7], form another widely studied ensemble [1–4, 8]. This network ensemble is characterized by a power-law degree distribution

$$p_k \propto k^{-\lambda}, \quad k \geq m, \quad (1)$$

where m is the minimum degree.

The primary difference between ER and SF networks lies in the tail of their degree distributions. In ER networks, node degrees are narrowly distributed around the mean. In contrast, the power-law degree distribution in SF networks allows the existence of high-degree nodes (hubs), introducing strong heterogeneity into the network structure. This heterogeneity profoundly affects both critical behavior and dynamical processes, with the exponent λ playing a crucial role [6–13].

To understand how structural heterogeneity influences critical behavior, one of the most extensively studied models is

percolation [14], which provides a prototypical framework for exploring the emergence of large-scale connectivity in network systems [15, 16]. In the bond percolation model, each link is independently occupied with probability P . As P increases, the system undergoes a percolation transition at a critical threshold P_c , above which a giant cluster emerges, containing a finite fraction of nodes connected by occupied bonds. This transition is accompanied by rich critical phenomena in the vicinity of P_c .

For SF networks, a well-known result is that for $2 < \lambda < 3$, the percolation threshold P_c vanishes; that is, even an infinitesimally small occupation probability results in a giant cluster. Moreover, larger λ values suppress the emergence of hubs, thereby reducing heterogeneity. When $\lambda > 4$, percolation on SF networks is generally believed to exhibit standard mean-field critical behavior, similar to ER networks [9, 17, 18]. However, for $\lambda < 4$, the critical exponents of percolation on SF networks remain under debate [19]. Various theoretical approaches suggested different values for critical exponents, particularly within the range $2 < \lambda < 3$. For instance, in this regime, the Fisher exponent τ for describing the cluster-size distribution has been reported as $(2\lambda - 3)/(\lambda - 2)$ [9] and λ [10, 20]. The correlation-length exponent ν has been predicted as either $(\lambda - 1)/(3 - \lambda)$ [9] or $2/(3 - \lambda)$ [21]. More intriguingly, a susceptibility-like quantity defined as $\chi \equiv \sum_{k>1} C_k^2/V$, where C_k is the size of the k th largest cluster and the sum is over all clusters excluding the largest one, is suggested to vanish at criticality for $2 < \lambda < 3$ [9]. This contradicts the standard percolation behavior in which χ diverges at criticality, typically following finite-size scaling (FSS) as $\chi \sim V^{2d_f-1}$, where d_f is the volume fractal dimension of percolation clusters.

While much attention has been given to the role of the degree exponent λ , FSS behavior on SF networks is also strongly affected by the degree cutoff K , which limits the maximum node degree [22]. The cutoff effectively tunes the heterogeneity of the network: smaller λ increases heterogeneity by allowing more hubs, whereas smaller K strictly restricts the presence of such hubs. Thus, the interplay between λ and K is expected to influence the structural heterogeneity of the network, which may, in turn, give rise to different FSS behav-

* lim@hfut.edu.cn

iors—though this relationship remains to be fully understood.

From extreme-value theory, even without an explicit upper bound K in the degree distribution of Eq. (1), the finite system size V naturally imposes a constraint on the maximum degree. This so-called *natural cutoff* can be estimated such that the expected number of nodes with degree larger than K remains finite as $V \rightarrow \infty$ [16, 22–24],

$$\int_K^V p_k dk \sim \mathcal{O}(1), \quad (2)$$

yielding the scaling [25],

$$K \sim V^{1/(\lambda-1)}. \quad (3)$$

This sets the intrinsic upper limit of the power-law degree distribution in Eq. (1). Even if a larger cutoff exponent is specified, the generated network will effectively revert to natural cutoff.

In real-world networks, however, degree cutoffs are often constrained by physical limits or design considerations, and are typically smaller than natural cutoff [26]. Nonetheless, they usually grow with system size according to

$$K \sim V^\kappa, \quad (4)$$

where the cutoff exponent κ ranges from 0 to 1. For $\kappa \rightarrow 1$, the cutoff significantly exceeds the average degree and allows for the presence of hubs; in contrast, when $\kappa \rightarrow 0$, the cutoff becomes finite and comparable to the average degree. A representative case is the *structural cutoff* $\kappa = 1/2$, i.e., $K \sim \sqrt{V}$, which arises in uncorrelated SF networks that forbid multiple links [23, 27–31]. In such networks, the maximum degree should not exceed this structural limit.

In this paper, we employ the percolation model to demonstrate that the FSS behaviors on SF networks depends not only on the degree exponent λ but also on the cutoff exponent κ . For $\lambda < 4$, the FSS behavior varies continuously with κ : when $\kappa \rightarrow 0$, standard mean-field behavior emerges regardless of λ . Thus, a crossover from the specialized critical behaviors of SF networks to the mean-field behavior can be observed for any λ by varying κ . In the regime $2 < \lambda < 3$, where the percolation threshold vanishes and conventional FSS becomes ill-defined, we show that proper FSS can still be observed near a dynamic pseudocritical point. In particular, the abnormal behaviors, such as the vanishing of susceptibility, can be mitigated by choosing small κ , thereby restoring a divergent susceptibility that satisfies the hyperscaling relation. For $\lambda > 4$, the system always exhibits mean-field criticality, with λ and κ affecting only the corrections to scaling.

The remainder of the paper is organized as follows. In Sec. II, we introduce the network and percolation models along with the simulation algorithms. In Sec. III, we present results on the FSS behavior with varying λ and κ . Finally, a discussion is included in Sec. IV.

II. MODEL AND ALGORITHM

A. Scale-free network

We consider percolation processes on SF networks generated by the configuration model [32, 33]. The network consists of V nodes, where each node i is assigned a degree k_i drawn independently from the power-law distribution $p_k \sim k^{-\lambda}$. To implement the degree cutoff, we employ the inverse transform sampling method with an explicit upper bound $K = aV^\kappa$ on the degree [34], where a is V -independent parameter. The minimum degree is set as $m = 2$ to ensure that the network is locally connected [35]. In most cases, we set $a = 1$; however, for small values of κ , we increase a to 2 or 4 so that the cutoff K remains sufficiently larger than the minimum degree m . After assigning degrees to all sites, we construct the network by randomly pairing the resulting half-edges (stubs) to form undirected links, while rejecting self-loops and multiple links. This yields an ensemble of SF networks with the target degree distribution.

To maintain randomness and the absence of self-loops and multiple links, the degree cutoff cannot be larger than the structural cutoff, i.e., $\kappa \leq 1/2$ [29, 30]. Consequently, the natural cutoff $V^{1/(\lambda-1)}$ cannot be achieved for $\lambda < 3$. In addition, when $\kappa > 1/(\lambda - 1)$, the degree cutoff always matches the natural cutoff, and κ no longer affects the results. In other cases, the degree heterogeneity of the network is determined jointly by the exponents λ and κ .

B. Bond Percolation

Standard bond percolation studies the formation of connected structures (clusters) in a network where each link is independently occupied with a given probability P . In this work, we adopt an equivalent dynamic link-insertion process to realize bond percolation. Specifically, starting from an empty network where all links are absent, one link is randomly selected and added at each discrete time step T , chosen from the set of links generated by the configuration model. For any time step T , the system corresponds to a bond percolation realization with an effective occupation probability $P = T/E$, where E is the total number of links in the network.

During the link-insertion process, we monitor the size of the largest cluster C_1 as a function of T , and define the one-step increment of C_1 as [36, 37]

$$\Delta C_1(T) = C_1(T + 1) - C_1(T). \quad (5)$$

As the process proceeds, ΔC_1 initially grows as small clusters begin to merge. Near the percolation threshold P_c , the merging of large clusters leads to a sharp increase in C_1 , resulting in a peak in ΔC_1 . After this peak, the growth of C_1 slows down as most nodes become part of the largest cluster. Therefore, the fraction of inserted links \mathcal{P}_V , corresponding to the time step of the maximum ΔC_1 , can be identified as a pseudocritical point of the system. Note that, \mathcal{P}_V varies from realizations to realizations, termed as *dynamic pseudocritical point*.

C. Sampled quantities

For each realization, we first generate a SF network with V nodes. Then, we apply the link-insertion process and identify the dynamic pseudocritical point \mathcal{P}_V . Various quantities are sampled at \mathcal{P}_V [38], including the size of the k th largest cluster C_k and the number \mathcal{N}_s of clusters of size s . For a number of realizations, we calculate the following observables

- The mean pseudocritical point $P_V \equiv \langle \mathcal{P}_V \rangle$.
- The standard deviation of the dynamic pseudocritical point $\sigma_V \equiv \sqrt{\langle \mathcal{P}_V^2 \rangle - \langle \mathcal{P}_V \rangle^2}$.
- The mean size of the k th largest cluster $C_k \equiv \langle C_k \rangle$.
- A susceptibility-like quantity $\chi \equiv \langle \sum_{k>1} C_k^2 \rangle / V$, where the sum runs over all the clusters with the largest one excluded.
- The cluster-number density $n(s, V) \equiv \langle \mathcal{N}_s \rangle / V$.

Here, $\langle \cdot \rangle$ denotes an ensemble average evaluated at \mathcal{P}_V , referred to as the event-based ensemble [39, 40].

III. NUMERICAL RESULTS

A. $2 < \lambda < 3$

1. Dynamic pseudocritical point

As shown by Molloy and Reed [33, 41], a giant component emerges in a network when the degree distribution satisfies $\langle k^2 \rangle / \langle k \rangle > 2$. Accordingly, the percolation threshold on SF networks is given by [32]

$$P_c = \frac{\langle k \rangle}{\langle k(k-1) \rangle} = \frac{\zeta(\lambda-1, m)}{\zeta(\lambda-2, m) - \zeta(\lambda-1, m)}, \quad (6)$$

where $\zeta(s, a) \equiv \sum_{n=0}^{\infty} (n+a)^{-s} = \sum_{n=a}^{\infty} n^{-s}$ is the Hurwitz zeta function, and m is the minimum degree.

For $2 < \lambda < 3$, the Hurwitz zeta function $\zeta(\lambda-2, m)$ diverges, resulting in a vanishing percolation threshold in the thermodynamic limit. Taking $\lambda = 2.5$ as an example, Fig. 1 (a) shows the pseudocritical point P_V as a function of system volume V for various degree cutoffs. A clear FSS behavior $P_V \sim V^{-1/\nu}$ is observed for all cutoffs, confirming that $P_V \rightarrow P_c = 0$ as $V \rightarrow \infty$. Moreover, the exponent $1/\nu$ systematically decreases with decreasing cutoff, indicating that although hubs still promote global connectivity and ensure $P_c = 0$, suppressing hub sizes amplifies finite-size effects and slows the convergence of P_V toward zero.

To quantitatively understand this behavior, we adopt a truncated power-law degree distribution ($m \leq k \leq K$) in Eq. (6). Using the asymptotic expansion of the Hurwitz zeta function [42], the critical point $P_c(K)$ for a given cutoff $K \sim V^\kappa$ behaves as

$$P_c(K) - P_c \propto \begin{cases} K^{3-\lambda} \sim V^{-\kappa(\lambda-3)}, & \lambda > 3, \\ (\ln K)^{-1} \sim (\ln V)^{-1}, & \lambda = 3, \\ K^{\lambda-3} \sim V^{-\kappa(3-\lambda)}, & 2 < \lambda < 3. \end{cases} \quad (7)$$

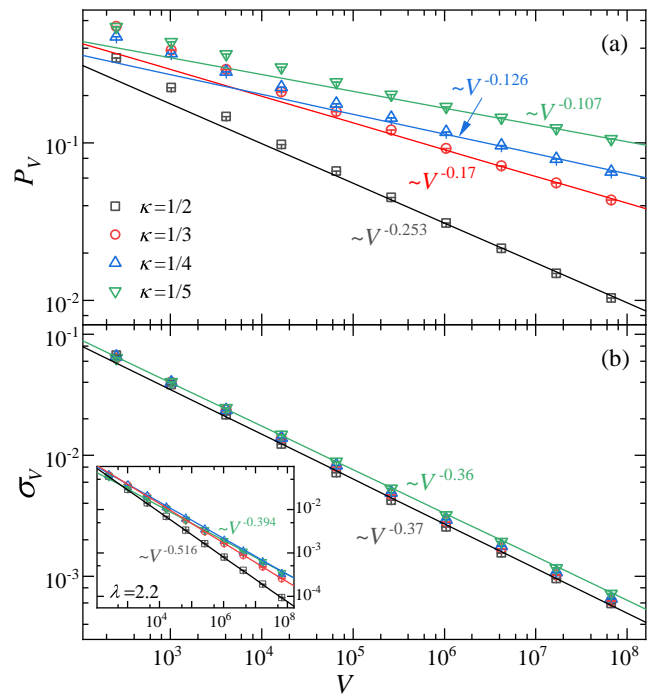


FIG. 1. (Color online) Asymptotic behaviors of dynamic pseudocritical points for $\lambda = 2.5$. (a) The mean pseudocritical point P_V is plotted against the system volume V for different degree cutoffs, demonstrating a clear power-law scaling $P_V \sim V^{-1/\nu}$. This indicates that for any degree cutoff, the SF network exhibits a vanishing percolation threshold. The fit results further suggest that the exponent $1/\nu$ decreases as the degree cutoff decreases. (b) The fluctuation σ_V of the dynamic pseudocritical point as a function of system volume V . The FSS of $\sigma_V \sim V^{-1/\nu'}$ implies a different exponent ν' , which appears insensitive to the cutoff exponent κ . The lines indicate the fit result $1/\nu' = 0.36$ and $1/\nu' = 0.37$. The inset shows $\sigma_V \sim V^{-1/\nu'}$ for $\lambda = 2.2$, suggesting the exponent ν' is still κ -dependent.

For natural cutoff, $\kappa = 1/(\lambda - 1)$, Eq. (7) recovers the result of Ref. [9]. For $2 < \lambda < 3$, the natural cutoff exceeds the structural cutoff $V^{1/2}$, and thus is not feasible for random SF networks without multiple links.

Equation (7) thus explains the numerical results in Fig. 1 (a): the scaling exponent $1/\nu = \kappa(3 - \lambda)$ decreases as κ decreases. To extract ν quantitatively, we perform least-squares fits of P_V as a function of V , applying a lower cutoff V_{\min} to evaluate the stability of fit. Accordingly, we adopt the following FSS ansatz

$$P_V = P_c + V^{-1/\nu}(a_0 + a_1 V^{-\omega}), \quad (8)$$

where ω is the leading correction-to-scaling exponent. In general, we select the smallest V_{\min} for which the reduced chi-square is close to unity and remains stable when increasing V_{\min} .

We note that quenched randomness and structural heterogeneity introduce strong finite-size corrections [43], which often prevent stable fits when ω is treated as a free parameter in Eq. (8). In such cases, we instead attempt a series of fits using fixed values of ω to identify a stable fitting result.

TABLE I. The fit results of the critical exponents for percolation on SF networks. The exponents $1/\nu'$ and d_f are extracted by fitting σ_V and C_1 to the FSS forms in Eqs. (10) and (11), respectively. For $\lambda = 3.5$, a logarithmic correction is included via Eq. (12) to obtain d_f . The percolation threshold P_c and exponent $1/\nu$ are obtained by fitting P_V to Eq. (8). For $2 < \lambda < 3$, the threshold vanishes ($P_c = 0$). For $\lambda = 3.3, 3.5, 3.8, 4.5$, and 6 , the thresholds given by Eq. (6) are $0.1730, 0.2687, 0.3889, 0.5901$, and 0.8135 , respectively. Missing entries indicate that stable fitting was not achievable under the corresponding parameters. Here, NC is an abbreviation for natural cutoff.

λ	κ	d_f	$1/\nu$	$1/\nu'$	P_c
2.2	1/2	0.39(1)	0.39(1)	0.516(8)	0.00001(3)
	1/3	0.500(5)	0.24(1)	0.448(4)	0.000(3)
	1/4	0.555(5)	0.18(1)	0.417(5)	0.005(5)
	1/5	0.588(6)	0.14(1)	0.394(6)	0.003(2)
2.5	1/2	0.413(7)	0.253(2)	0.37(1)	0.00002(5)
	1/3	0.511(6)	0.17(1)	0.36(1)	-0.001(2)
	1/4	0.558(6)	0.126(7)	0.36(1)	-0.004(4)
	1/5	0.585(4)	0.107(5)	0.36(1)	0.000(9)
	1/6	0.60(1)	0.086(6)	0.36(1)	0.00(1)
2.8	1/2	0.462(5)	0.11(2)	0.17(2)	-0.002(3)
	1/3	0.533(5)	0.07(3)	0.28(1)	0.00(2)
	1/4	0.57(1)	0.07(3)	0.32(1)	0.02(2)
	1/5	0.588(4)	–	0.32(1)	–
	1/6	0.60(1)	–	0.33(1)	–
3.3	NC	0.564(4)	0.14(2)	0.18(2)	0.173(3)
3.5	NC	0.60(1)	0.19(2)	0.21(1)	0.271(3)
	1/3	0.60(1)	0.17(1)	0.24(1)	0.269(2)
	1/4	0.61(1)	0.14(3)	0.27(1)	0.269(6)
	1/5	0.618(7)	0.11(1)	0.28(1)	0.26(1)
	1/6	0.62(1)	–	0.29(1)	–
	1/8	0.633(4)	–	0.30(1)	–
3.8	NC	0.620(8)	0.27(1)	0.26(2)	0.391(1)
4.5	NC	0.67(2)	0.32(1)	0.33(1)	0.5908(1)
	1/4	0.668(4)	0.33(1)	0.33(2)	0.590(1)
	1/5	0.667(6)	0.33(1)	0.33(2)	0.5906(3)
6	NC	0.666(2)	0.333(5)	0.33(1)	0.8135(1)
	1/6	0.666(1)	0.33(1)	0.326(5)	0.8135(2)

However, due to the lack of a theoretical basis for selecting ω , the final estimates represent an overall consideration of these fits, limiting the precision of the extracted exponents. In some instances, the fitting results vary significantly with different fixed ω , so that no stable and consistent estimate can be obtained with the current data and the fit function. Nevertheless, this limitation may be overcome in future studies with access to larger-scale simulations, which are beyond our current computational capability.

The fitted values of $1/\nu$ are summarized in Table I. For $2 < \lambda < 3$, we present results for $\lambda = 2.2, 2.5$, and 2.8 , where the extracted values of $1/\nu$ agree with the theoretical prediction $1/\nu = \kappa(3 - \lambda)$ within one or two error bars. As λ approaches 3, the exponent $1/\nu = \kappa(3 - \lambda)$ becomes increasingly small, and Eq. (7) suggests a logarithmic asymptotic be-

havior. In such cases, a stable fit using Eq. (8) becomes more difficult. Indeed, for $\lambda = 2.8$, the fitted values of $1/\nu$ are systematically larger than the predicted ones, and for small κ , we are unable to obtain stable and consistent fits due to strong finite-size corrections and the limited range of system sizes accessible in our simulations. Nevertheless, the overall trend that $1/\nu$ decreases with decreasing κ remains robust.

The percolation threshold P_c is also estimated in the fitting procedure (see Table I). In the range $2 < \lambda < 3$, the estimated P_c is consistent with zero within at most two error bars. These results suggest that a vanishing threshold remains compatible with the data, although strong finite-size effects may obscure the asymptotic behavior.

In the limit $\kappa \rightarrow 0$, where the degree cutoff becomes independent of system size, the SF network effectively reduces to a configuration model with a fixed maximum degree. In this regime, the system is expected to exhibit mean-field percolation behavior with $\nu = 3$. However, within the range of κ accessible to our simulations, the fitted values of $1/\nu$ continue to decrease monotonically with decreasing κ , and can even fall below the mean-field value $1/3$. This indicates that $1/\nu$ may exhibit a sharp crossover from a vanishing value predicted by Eq. (7) to the mean-field value, as $\kappa \rightarrow 0$, rather than varying smoothly. Whether this crossover is truly discontinuous or smoothed out in the infinite-size limit remains an open question, requiring simulations on larger systems beyond current computational capabilities.

To further characterize the asymptotic behavior of dynamic pseudocritical points, we examine the standard deviation σ_V of \mathcal{P}_V . Figure 1 (b) shows σ_V versus V , revealing an FSS behavior of the form

$$\sigma_V \sim V^{-1/\nu'}. \quad (9)$$

For most of the percolation systems, it is known that $\nu' = \nu$ [44], implying that the pseudocritical shift and its fluctuations vanish at the same rate. However, fitting σ_V using the FSS ansatz

$$\sigma_V = V^{-1/\nu'}(a_0 + a_1 V^{-\omega}), \quad (10)$$

reveals that ν' is systematically smaller than ν , i.e., $\nu' < \nu$.

More intriguingly, in contrast to $1/\nu$, which systematically decreases with decreasing degree cutoff, the exponent $1/\nu'$ shows a nontrivial and λ -dependent trend: it increases for $\lambda = 2.8$, decreases for $\lambda = 2.2$, and remains nearly unchanged for $\lambda = 2.5$, as shown in Table I and Fig. 1 (b). This seemingly irregular behavior can be understood as a convergence toward the mean-field value. In the limit $\kappa \rightarrow 0$, the percolation on SF networks should follow the mean-field behavior with $\nu' = \nu = 3$. Therefore, as the cutoff decreases, $1/\nu'$ approaches the mean-field value $1/3$ from above or below, depending on its initial deviation – decreasing if initially larger than $1/3$, increasing if smaller. This convergence is clearly illustrated in the inset of Fig. 2, which shows $1/\nu'$ as a function of κ .

Furthermore, similar discrepancies between ν' and ν have been observed in high-dimensional percolation with open boundaries [44]. In this case, it has been argued that ν' , rather

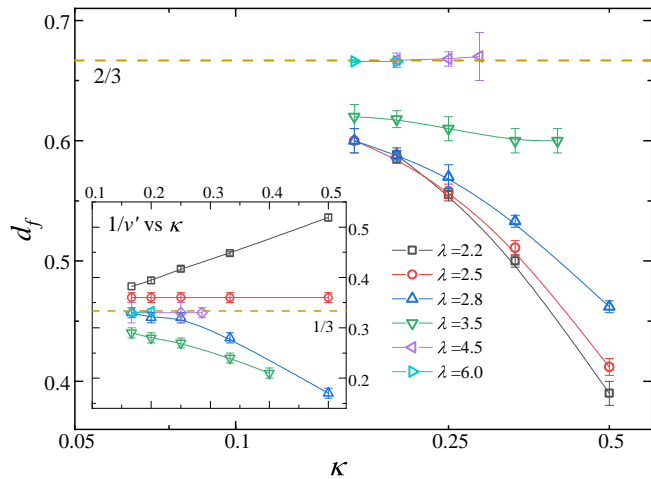


FIG. 2. (Color online) The fitted fractal dimension d_f as a function of the cutoff exponent κ for different λ . The scatters represent the results in Table I, and golden dashed line indicates the mean-field value $d_f = 2/3$. The inset shows the exponent $1/v'$ in Table I as a function of κ , where the golden dashed line is also for the mean-field value $v' = 3$. The plot demonstrate the trend that both d_f and v' converge towards the mean-field values for $\kappa \rightarrow 0$.

than ν , captures the true correlation-length scaling. Accordingly, we argue that for SF networks as well, ν does not represent the correlation-length exponent; instead, ν' should be taken as the correct one. More evidences for this argument will be demonstrated in the following sections.

2. Fractal dimension

For $2 < \lambda < 3$, the percolation threshold P_c vanishes, and hence at $P_c = 0$, only isolated sites exist regardless of system size. As a result, FSS behaviors cannot be observed at P_c . To overcome this difficulty, we investigate the FSS behaviors at the dynamic pseudocritical point \mathcal{P}_V , i.e., within the event-based ensemble.

Figure 3 (a) shows the mean size of the largest cluster C_1 , sampled at \mathcal{P}_V , as a function of V for $\lambda = 2.5$. A clear power-law scaling $C_1 \sim V^{d_f}$ is observed, where d_f denotes the volume fractal dimension. This result indicates that the percolation transition and associated FSS can still be well-defined in the regime $2 < \lambda < 3$ when data are sampled at the dynamic pseudocritical point, even though the subcritical phase is absent in the thermodynamic limit.

To estimate d_f , we fit C_1 using the FSS ansatz

$$C_1 = V^{d_f}(a_0 + a_1 V^{-\omega}). \quad (11)$$

The fitting results for different λ and κ are summarized in Table I. We find that the fractal dimension d_f depends on both λ and κ , with smaller cutoffs leading to larger d_f . This suggests that suppressing hubs (large λ or small κ) enhances connectivity among non-hub nodes, resulting in denser and more homogeneous cluster structures (large d_f). In addition, the mean-

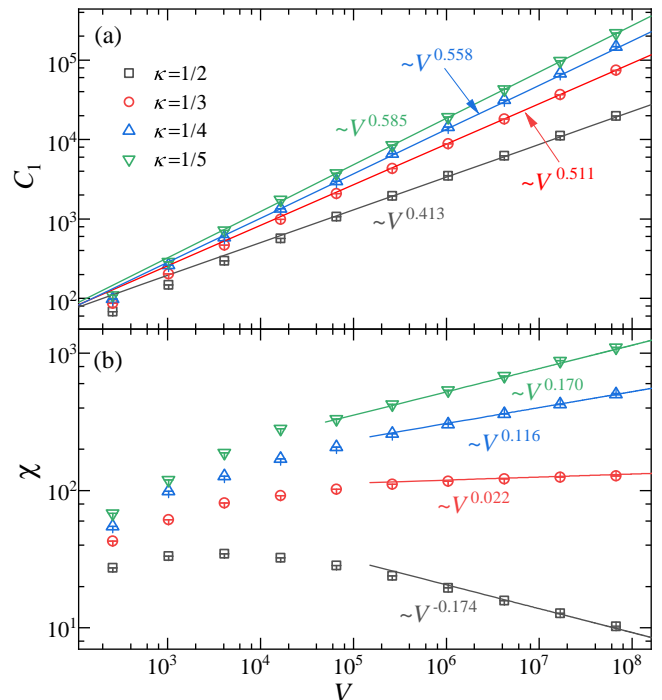


FIG. 3. (Color online) The FSS behaviors of the size of the largest cluster C_1 and the susceptibility-like quantity χ for $\lambda = 2.5$. (a) C_1 as a function of the system volume V for different degree cutoffs. The lines indicate the scaling $C_1 \sim V^{d_f}$, where d_f is the fitted fractal dimension listed in Table I. (b) χ as a function of V for different degree cutoffs. The lines indicate the scaling $\chi \sim V^{2d_f-1}$, with d_f from Table I.

field value $d_f = 2/3$ should be covered for $\kappa \rightarrow 0$, which is well demonstrated in Fig. 2.

For percolation, the susceptibility-like quantity χ is expected to diverge at criticality as a scaling form of $\chi \sim V^{2d_f-1}$. However, previous studies [9] have shown that χ vanishes at criticality for $2 < \lambda < 3$. As shown in Fig. 3 (b), for a large cutoff ($\kappa = 1/2$), we indeed observe a power-law decay of χ with increasing system volume, indicating a suppression of critical fluctuations. This vanishing susceptibility can be attributed to fluctuation localization: in scale-free networks with $2 < \lambda < 3$ and large degree cutoffs, a small number of hubs dominate the connectivity. The giant cluster forms primarily via connections to these hubs, rather than through the merging of many intermediate-sized clusters. Consequently, critical fluctuations are localized around these hubs, and the extended fluctuations necessary for a divergent are suppressed, with this effect becoming more pronounced as the system size increases. In contrast, for smaller values of κ , the influence of hubs diminishes, and χ recovers the typical divergence expected in standard percolation transitions, see Fig. 3 (b).

Furthermore, the lines in Fig. 3 (b) represent the standard scaling form $\chi \sim V^{2d_f-1}$, using d_f obtained from fitting $C_1 \sim V^{d_f}$ (Table I). The excellent agreement between the simulation results and the predicted scaling, even for $\kappa = 1/2$ where $d_f < 0.5$ and thus $2d_f - 1 < 0$, confirms the validity of the

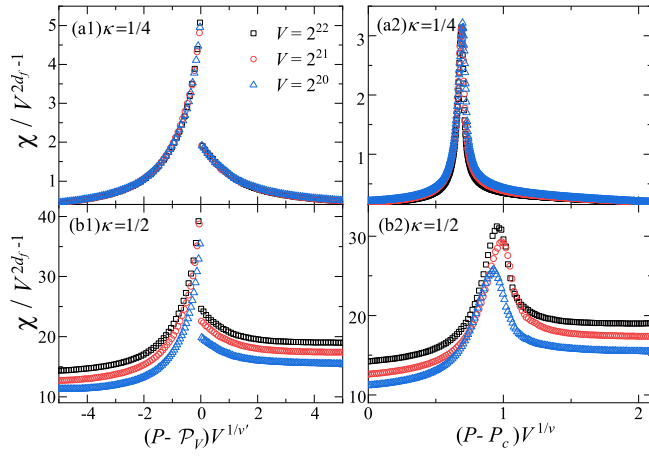


FIG. 4. (Color online) The FSS behavior of the susceptibility-like quantity χ near the dynamic pseudocritical point \mathcal{P}_V and the critical point P_c for $\lambda = 2.5$. Panels (a1) and (a2) show χ/V^{2d_f-1} as a function of $(P - \mathcal{P}_V)V^{1/v'}$ and $(P - P_c)V^{1/v}$, respectively, for $\kappa = 1/4$, where χ diverges. A better data collapse is observed in (a1), supporting the applicability of standard FSS theory around the pseudocritical point \mathcal{P}_V . Panels (b1) and (b2) show the same rescaled plots for $\kappa = 1/2$, where χ vanishes in the thermodynamic limit. Data collapse cannot be achieved for both (b1) and (b2), suggesting an abnormal FSS. The exponents used here are taken from the fit results in Table I. For (a1) and (b1), the discontinuity of χ at \mathcal{P}_V comes from the event-based definition of \mathcal{P}_V .

scaling relation between C_1 and χ across different κ values.

By applying standard FSS theory around \mathcal{P}_V , the behaviors of the susceptibility χ are represented as $\chi = V^{2d_f-1}\tilde{\chi}(x)$, where $x \equiv (P - \mathcal{P}_V)V^{1/v'}$ or $x \equiv (P - P_c)V^{1/v}$. To demonstrate this FSS behavior, we plot the rescaled susceptibility χ/V^{2d_f-1} as a function of $(P - \mathcal{P}_V)V^{1/v'}$ for $\kappa = 1/4$ in Fig. 4 (a1). By using the fitted values of d_f and $1/v'$ from Table I, the data for different system sizes collapse remarkably well near \mathcal{P}_V . The discontinuity of χ at \mathcal{P}_V comes from the event-based definition of \mathcal{P}_V . In contrast, as shown in Fig. 4 (a2), the same rescaling near P_c using $x = (P - P_c)V^{1/v}$ cannot produce a satisfactory data collapse as that in Fig. 4 (a1). These results not only supports the reliability of our extracted exponents d_f and v' , but also indicates that the standard FSS theory is applicable around the dynamic pseudocritical point \mathcal{P}_V , with v' playing the role of the correlation-length exponent instead of v .

For cases where the susceptibility vanishes in the thermodynamic limit (e.g., $\kappa = 1/2$), the rescaled susceptibility χ/V^{2d_f-1} exhibits a converging height across different system sizes as $P \rightarrow \mathcal{P}_V$, consistent with the FSS behavior observed in Fig. 3 (b). However, away from \mathcal{P}_V , a data collapse cannot be achieved, indicating that the scaling form holds only locally at \mathcal{P}_V . As shown in Fig. 4 (b2), the rescaling with $x = (P - P_c)V^{1/v}$ also fails to produce a collapse in the whole range of x . Moreover, despite the theoretical result $P_c = 0$ for $2 < \lambda < 3$, the peak of χ in both Figs. 4 (b1) and (b2) does not show an asymptotic shift toward $P_c = 0$ as system size increases. These findings suggest that while standard FSS holds

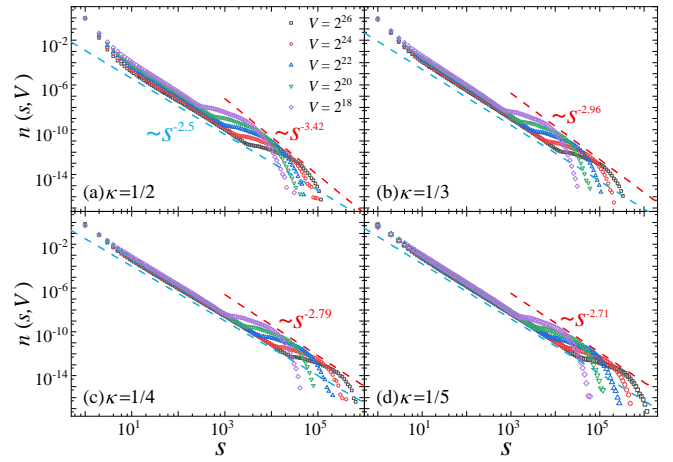


FIG. 5. (Color online) Cluster-number density $n(s, V)$ for $\lambda = 2.5$ across different system volumes and degree cutoffs. Due to the vanishing percolation threshold in this regime, $n(s, V)$ decreases with increasing system size for all $s > 1$. Red dashed lines show power-law decay with exponent $\tau' = 1 + 1/d_f$, where the κ -dependent d_f is obtained from the scaling of C_1 in Fig. 3 (a). Blue dashed lines correspond to the Fisher exponent $\tau = \lambda$.

near \mathcal{P}_V , the overall scaling behavior for $2 < \lambda < 3$ exhibits certain anomalies that cannot be fully captured by conventional FSS functions. This highlights the intrinsic complexity of FSS in systems with vanishing thresholds and strong structural heterogeneity.

3. Cluster-number density

At the critical point, percolation clusters are expected to be self-similar, with the cluster-number density following the scaling form $n(s, V) = s^{-\tau}\tilde{n}(s/V^{d_f})$, where hyperscaling predicts the Fisher exponent $\tau = 1 + 1/d_f$. However, for $2 < \lambda < 3$, the percolation threshold vanishes in the thermodynamic limit, and only isolated sites remain. Even at the dynamic pseudocritical point, the cluster-number density $n(s, V)$ for $s > 1$ decreases with increasing system size V , as demonstrated in Fig. 5.

Nevertheless, Fig. 5 reveals a clear dependence of $n(s, V)$ on the degree cutoff. First, a power-law decay of $n(s, V)$ is still visible for large s (red dashed lines), with an exponent consistent with the hyperscaling relation $\tau' = 1 + 1/d_f$, where d_f is extracted from the scaling of C_1 in Fig. 3 (a). Second, although the overall magnitude of $n(s, V)$ decreases for $V \rightarrow \infty$, a Fisher exponent τ can still be roughly identified (blue dashed lines). Remarkably, this exponent appears to be independent of the degree cutoff and aligns with the theoretical prediction $\tau = \lambda$ from the Potts model mapping [10] or the asymptote of the cluster-size distribution [20]. This finding deviates from the earlier mean-field result $\tau = (2\lambda - 3)/(\lambda - 2)$ [9], which gives $\tau = 4$ for $\lambda = 2.5$ – clearly inconsistent with the numerical data in Fig. 5.

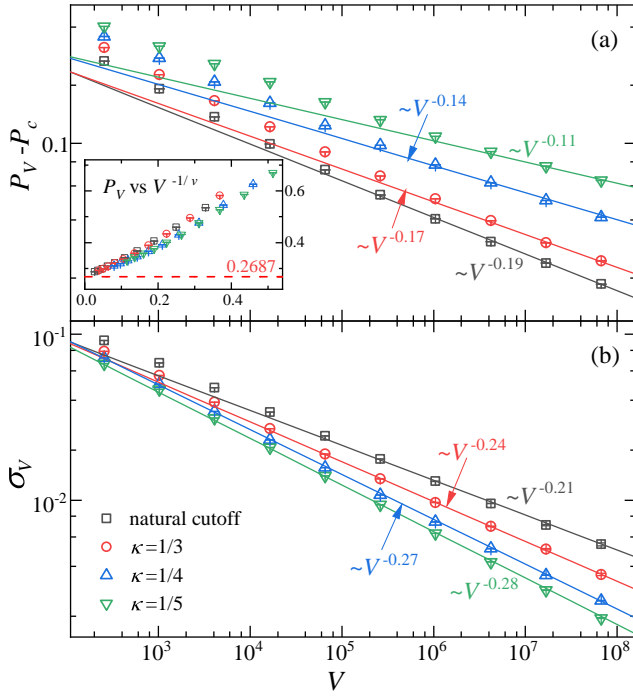


FIG. 6. (Color online) Asymptotic behavior of dynamic pseudocritical points for $\lambda = 3.5$. (a) The distance $P_V - P_c$ between the critical point P_c and the dynamic pseudocritical point P_V is plotted against system volume V for various degree cutoffs. The results exhibit clear power-law scaling $P_V - P_c \sim V^{-1/\nu}$ for large V , with the scaling exponent $1/\nu$ decreasing as the cutoff becomes smaller. The inset shows P_V versus $V^{-1/\nu}$, where all curves extrapolate to the same $P_c \approx 0.2687$ as $V^{-1/\nu} \rightarrow 0$, indicating that the critical point is independent of the degree cutoff. (b) Fluctuation σ_V of the dynamic pseudocritical point as a function of V . The FSS $\sigma_V \sim V^{-1/\nu'}$ yields a different exponent $1/\nu'$, which increases as κ decreases.

B. $3 < \lambda < 4$

1. Dynamic pseudocritical points

For $3 < \lambda < 4$, the Hurwitz zeta function $\zeta(s, a)$ in Eq.(6) is finite, yielding a nontrivial percolation threshold $P_c > 0$. Table I lists the fitted values of P_c for $\lambda = 3.3, 3.5$, and 3.8 , obtained by fitting P_V using the FSS ansatz in Eq. (8). These values are consistent with the theoretical prediction from Eq. (6). Notably, the percolation threshold given by Eq. (6) is independent of the cutoff exponent κ , since $K \sim V^\kappa$ diverges for any $\kappa > 0$.

In contrast, the exponent $1/\nu$ governing the convergence $P_c - P_V \sim V^{-1/\nu}$ is κ -dependent, as illustrated in Fig. 6 (a). The fitted values of $1/\nu$, also listed in Table I, agree well with the theoretical expression $1/\nu = \kappa(\lambda - 3)$ from Eq. (7), which reduces to $1/\nu = (\lambda - 3)/(\lambda - 1)$ under the natural cutoff [9, 45]. Plotting P_V versus $V^{-1/\nu}$ in the inset of Fig. 6 (a) confirms that all curves converge to the same critical point P_c as $V^{-1/\nu} \rightarrow 0$, further validating the predicted exponent and percolation threshold.

A similar scaling behavior is observed for the fluctuation

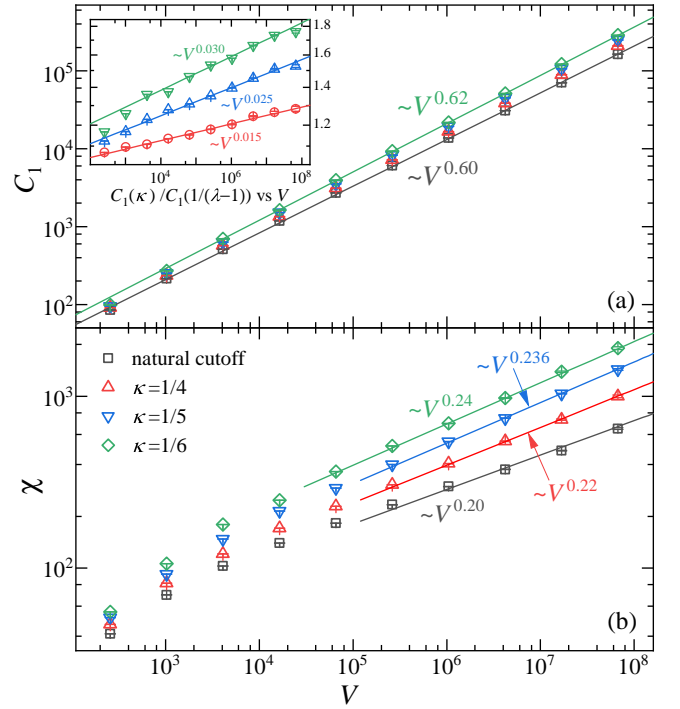


FIG. 7. (Color online) The FSS behaviors of the percolation on SF networks with $\lambda = 3.5$. (a) The largest-cluster size C_1 as a function of system volume V for various degree cutoffs. The lines indicate the scaling $C_1 \sim V^{d_f}$ for natural cutoff $\kappa = 1/(\lambda - 1)$ and $\kappa = 1/6$, respectively, with fitted fractal dimensions d_f listed in Table I. The inset shows $C_1(\kappa)/C_1(1/(\lambda - 1))$ for different κ . The nice scalings for large V indicate that different κ values lead to distinct fractal dimensions from that of natural cutoff. (b) χ as a function of V for different degree cutoffs. The lines represent the scaling $\chi \sim V^{2d_f - 1}$, using d_f from Table I.

$\sigma_V \sim V^{-1/\nu'}$, as shown in Fig. 6 (b) for $\lambda = 3.5$, with the fitted exponents $1/\nu'$ summarized in Table I. Under the natural cutoff, we find $1/\nu' = 1/\nu = (\lambda - 3)/(\lambda - 1)$, in agreement with the theoretical prediction. Since $1/\nu' = (\lambda - 3)/(\lambda - 1)$ exceeds the mean-field value $1/3$ for $3 < \lambda < 4$, the exponent $1/\nu'$ decreases toward $1/3$ as the cutoff becomes more stringent (i.e., smaller κ), as illustrated in the inset of Fig. 2. This trend echoes the crossover behavior discussed earlier for the regime $2 < \lambda < 3$.

2. Critical clusters

According to the theoretical values of the critical exponents $\beta = 1/(\lambda - 3)$ and $1/\nu = (\lambda - 3)/(\lambda - 1)$ from Ref. [9], the volume fractal dimension of the largest cluster at criticality can be derived from the hyperscaling relation $d_f = 1 - \beta/\nu = (\lambda - 2)/(\lambda - 1)$, implying a λ -dependent fractal structure. For $\lambda = 3.3, 3.5$, and 3.8 , this yields $d_f \approx 0.565, 0.6$, and 0.643 , respectively, in good agreement with the fitted values listed in Table I.

For a smaller degree cutoff, a clear power-law scaling $C_1 \sim V^{d_f}$ is still observed, as shown in Fig. 7 (a) for $\lambda = 3.5$. The

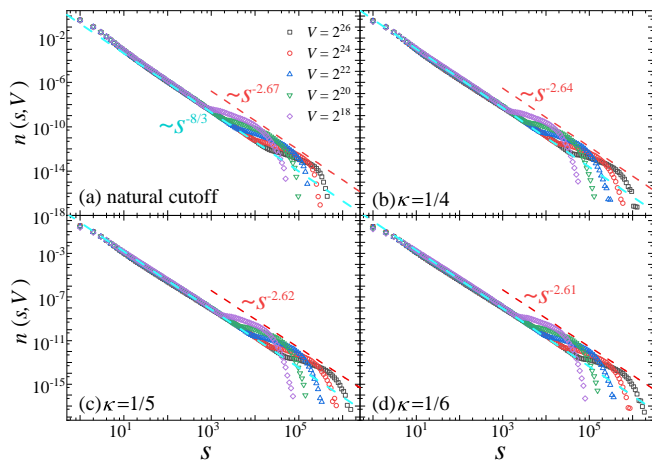


FIG. 8. (Color online) Cluster number density $n(s, V)$ for $\lambda = 3.5$ across different system volumes and degree cutoffs. Blue dashed lines indicate the Fisher exponent $\tau = (2\lambda - 3)/(\lambda - 2) = 8/3$. Red dashed lines show power-law decay with exponent $\tau' = 1 + 1/d_f$, where the κ -dependent d_f is obtained from the FSS of C_1 in Fig. 7 (a). These results show that while the bulk of $n(s, V)$ is governed by λ -dependent scaling, the tail is also influenced by the degree cutoff.

inset further demonstrates that the ratio $C_1(\kappa)/C_1(1/(\lambda - 1))$ grows as a power law when $\kappa < 1/(\lambda - 1)$, confirming that d_f increases with decreasing κ . This indicates that the fractal dimension depends on both λ and κ , and increases (i.e., becomes more compact) as hub nodes are more strongly suppressed, consistent with the trend observed for $2 < \lambda < 3$. In the limit $\kappa \rightarrow 0$, where the degree cutoff becomes very restrictive, the influence of the SF topology vanishes, and d_f approaches the mean-field value $2/3$. This asymptotic behavior is clearly demonstrated in Fig. 2.

Moreover, the susceptibility-like quantity χ is found to scale as $\chi \sim V^{2d_f - 1}$, consistent with FSS theory for percolation. As shown in Fig. 7 (b), simulation data for large systems follow this scaling law, using the d_f values extracted from C_1 , further supporting the internal consistency of the FSS framework for $3 < \lambda < 4$.

The κ -dependent fractal dimension also implies a κ -dependent Fisher exponent $\tau' = 1 + 1/d_f$. However, as in the regime $2 < \lambda < 3$, this exponent characterizes only the hump in the tail of the cluster-size distribution $n(s, V)$, as shown in Fig. 8. The bulk of $n(s, V)$ is instead governed by the theoretical value $\tau = (2\lambda - 3)/(\lambda - 2)$ [9, 10], which remains independent of the degree cutoff.

C. $\lambda > 4$

For $\lambda > 4$, percolation on SF networks exhibits standard mean-field behavior, with $d_f = 2/3$ and $1/\nu = 1/\nu' = 1/3$. No crossover is expected in this regime. As shown in Table I, for $\lambda = 6$, both the natural cutoff and a cutoff with $\kappa = 1/6$ yield d_f and $1/\nu$ values consistent with the mean-field predictions within error bars.

As λ approaches 4, for instance at $\lambda = 4.5$, the fitted d_f

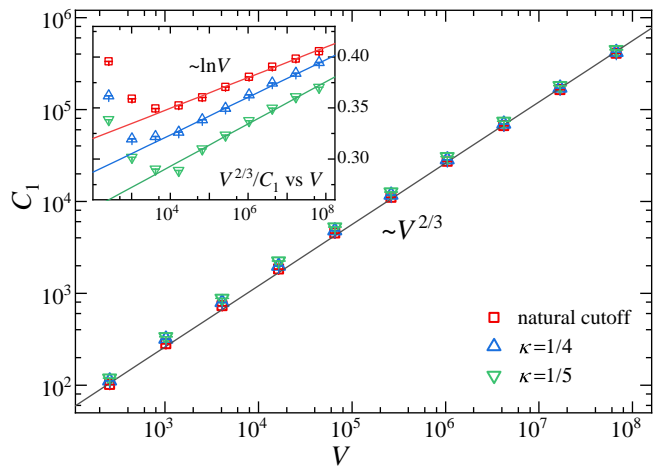


FIG. 9. (Color online) The FSS of $C_1 \sim V^{d_f}$ across different degree cutoff for $\lambda = 4.5$. The line shows the scaling of $C_1 \sim V^{2/3}$. The inset plots the data of $V^{2/3}/C_1$ as a function of V in a semi-logarithmic plot. For large V , the curve of $C_1/V^{2/3}$ approaches a straight line in the semi-logarithmic plot, suggesting a scaling behavior $V^{2/3}/C_1 \sim \ln V$, i.e., the FSS of C_1 contains a multiplicative logarithmic correction.

values from Eq. (11) are slightly below $2/3$, yielding $d_f \approx 0.64$ – 0.65 . However, as illustrated in Fig. 9, the asymptotic scaling $C_1 \sim V^{2/3}$ appears to hold for large V , independent of κ . To examine this deviation, we plot $V^{2/3}/C_1$ versus V on a semi-log scale (inset of Fig. 9). The data form an approximately straight line at large V , indicating $V^{2/3}/C_1 \sim \ln V$, and suggesting that logarithmic corrections accompany the scaling as $\lambda \rightarrow 4$.

To account for this, we incorporate a logarithmic term into the FSS ansatz

$$C_1 = V^{d_f} (\ln V + b)^X (a_0 + a_1 V^{-\omega}). \quad (12)$$

Allowing all parameters to vary freely yields unstable fits. Fixing $X = 1$ and testing various combinations of fixed b and ω , we obtain consistent estimates of d_f across different κ values, all converging to the mean-field value $2/3$ (Table I). The reported error bars reflect the spread among these combinations.

IV. DISCUSSION

In this work, we systematically study the bond-percolation transitions on SF networks with tunable degree cutoffs. By analysing the FSS behaviors of the dynamic pseudocritical points \mathcal{P}_V , the largest-cluster size C_1 , and the susceptibility-like quantity χ , we demonstrated that the FSS behavior depends in a non-trivial way on both the degree exponent λ and the cutoff exponent κ . Standard mean-field exponents reemerge whenever either $\lambda \geq 4$ or $\kappa \rightarrow 0$. The kernel of these crossovers is a structural change from heterogeneity to uniformity that underlines the pivotal role of hub nodes: suppressing hubs reduces network heterogeneity and drives the system towards the behavior of homogeneous or random graphs.

Based on extensive simulations, we summarize the FSS behavior as follows. For $\lambda > 4$, the system consistently exhibits mean-field behavior, regardless of λ or κ . For $2 < \lambda < 4$, the fractal dimension d_f , the critical exponents ν (describing the shift of \mathcal{P}_V from P_c), and ν' (describing the fluctuation of \mathcal{P}_V) all depend on κ and deviate from their mean-field values. In contrast, except $\kappa = 0$, for which the Fisher exponent takes the mean-field value $\tau = 5/2$, it is determined solely by λ , consistent with the relations $\tau = \lambda$ for $2 < \lambda < 3$ and $\tau = (2\lambda - 3)/(\lambda - 2)$ for $3 < \lambda < 4$. In the case of the natural cutoff, our results support $\nu = \nu' = (\lambda - 1)/|\lambda - 3|$, and d_f is consistent with the hyperscaling relation $\tau = 1 + 1/d_f$. As κ decreases, ν and ν' become distinct: ν' increases or decreases toward the mean-field value $\nu' = 3$, while ν increases above 3 before shifting to $\nu = 3$ at $\kappa = 0$. Meanwhile, the fractal dimension d_f increases continuously toward the mean-field value $2/3$.

These crossover phenomena raise several open questions. First, in SF networks, intrinsic degree correlations may change alongside variations in the degree cutoff [30, 46]. Meanwhile, deliberately imposed correlations are known to alter percolation universality classes [24, 47, 48]. Can the effects of a varying cutoff be understood as manifestations of intrinsic correlation changes, and might both be captured within a unified framework? Second, the degree distribution

of empirical SF networks is often truncated in the form of an exponential decay [26], rather than by a hard cutoff. How such exponentially suppressed cutoffs influence the FSS behavior remains an open question. Third, although both ν and ν' vary with λ and κ , our results consistently show $\nu > \nu'$, a relation also observed in high-dimensional percolation with open boundaries [44, 49]. This resemblance suggests that both systems may share underlying organizational mechanisms yet to be uncovered. Fourth, our simulations reveal that SF networks exhibit strong finite-size corrections, often with mixed logarithmic contributions. These effects complicate the FSS analysis and call for more refined tools, such as the recently proposed gap method [50], which offers a promising way to capture more clean FSS. Overall, addressing these questions will require new theoretical insights, improved scaling arguments, and large-scale simulations that jointly consider degree heterogeneity, cutoff effects, and correlation structures.

ACKNOWLEDGMENTS

The research was supported by the Fundamental Research Funds for the Central Universities (No. JZ2023HGTO220).

-
- [1] S. N. Dorogovtsev, A. V. Goltsev, and J. F. F. Mendes, Critical phenomena in complex networks, *Rev. Mod. Phys.* **80**, 1275 (2008).
 - [2] Z. Burda, J. D. Correia, and A. Krzywicki, Statistical ensemble of scale-free random graphs, *Phys. Rev. E* **64**, 046118 (2001).
 - [3] S. Dorogovtsev, J. Mendes, and A. Samukhin, Principles of statistical mechanics of uncorrelated random networks, *Nucl. Phys. B* **666**, 396 (2003).
 - [4] J. Park and M. E. J. Newman, Statistical mechanics of networks, *Phys. Rev. E* **70**, 066117 (2004).
 - [5] B. Bollobás, *Random Graphs*, 2nd ed. (Cambridge University Press, 2001).
 - [6] A.-L. Barabási, Scale-free networks: A decade and beyond, *Science* **325**, 412 (2009).
 - [7] A.-L. Barabási, *Network science* (Cambridge university press, 2016).
 - [8] A. V. Goltsev, S. N. Dorogovtsev, and J. F. F. Mendes, Critical phenomena in networks, *Phys. Rev. E* **67**, 026123 (2003).
 - [9] R. Cohen, D. ben Avraham, and S. Havlin, Percolation critical exponents in scale-free networks, *Phys. Rev. E* **66**, 036113 (2002).
 - [10] D.-S. Lee, K.-I. Goh, B. Kahng, and D. Kim, Evolution of scale-free random graphs: Potts model formulation, *Nucl. Phys. B* **696**, 351 (2004).
 - [11] C. Castellano and R. Pastor-Satorras, Non-mean-field behavior of the contact process on scale-free networks, *Phys. Rev. Lett.* **96**, 038701 (2006).
 - [12] H. Hong, M. Ha, and H. Park, Finite-size scaling in complex networks, *Phys. Rev. Lett.* **98**, 258701 (2007).
 - [13] S. Boccaletti, V. Latora, Y. Moreno, M. Chavez, and D.-U. Hwang, Complex networks: Structure and dynamics, *Phys. Rep.* **424**, 175 (2006).
 - [14] D. Stauffer and A. Aharony, *Introduction to percolation theory*, 2nd ed. (Taylor & Francis, London, 1991).
 - [15] M. E. J. Newman, *Networks: An Introduction* (Oxford University Press, 2010).
 - [16] M. Li, R.-R. Liu, L. Lü, M.-B. Hu, S. Xu, and Y.-C. Zhang, Percolation on complex networks: Theory and application, *Phys. Rep.* **907**, 1 (2021).
 - [17] S. N. Dorogovtsev, A. V. Goltsev, and J. F. F. Mendes, Ising model on networks with an arbitrary distribution of connections, *Phys. Rev. E* **66**, 016104 (2002).
 - [18] M. Leone, A. Vázquez, A. Vespignani, and R. Zecchina, Ferromagnetic ordering in graphs with arbitrary degree distribution, *Eur. Phys. J. B* **28**, 191 (2002).
 - [19] L. Cirigliano, G. Timár, and C. Castellano, Scaling and universality for percolation in random networks: A unified view, *Phys. Rev. E* **110**, 064303 (2024).
 - [20] I. Kryven, General expression for the component size distribution in infinite configuration networks, *Phys. Rev. E* **95**, 052303 (2017).
 - [21] F. Radicchi and C. Castellano, Breaking of the site-bond percolation universality in networks, *Nat. Commun.* **6**, 10196 (2015).
 - [22] C. Castellano and R. Pastor-Satorras, Routes to thermodynamic limit on scale-free networks, *Phys. Rev. Lett.* **100**, 148701 (2008).
 - [23] B. Waclaw, L. Bogacz, and W. Janke, Approaching the thermodynamic limit in equilibrated scale-free networks, *Phys. Rev. E* **78**, 061125 (2008).
 - [24] L.-H. Wang and Y.-M. Du, Percolating critical window for correlated scale-free networks, *Physica A* **664**, 130441 (2025).
 - [25] R. Cohen, K. Erez, D. ben Avraham, and S. Havlin, Breakdown of the internet under intentional attack, *Phys. Rev. Lett.* **86**, 3682 (2001).

- [26] A. Clauset, C. R. Shalizi, and M. E. J. Newman, Power-law distributions in empirical data, *SIAM Rev.* **51**, 661 (2009).
- [27] F. Chung and L. Lu, Connected components in random graphs with given expected degree sequences, *Ann. Comb.* **6**, 125 (2002).
- [28] Z. Burda and A. Krzywicki, Uncorrelated random networks, *Phys. Rev. E* **67**, 046118 (2003).
- [29] M. Boguñá, R. Pastor-Satorras, and A. Vespignani, Cut-offs and finite size effects in scale-free networks, *Eur. Phys. J. B* **38**, 205 (2004).
- [30] J.-S. Lee, K.-I. Goh, B. Kahng, and D. Kim, Intrinsic degree-correlations in the static model of scale-free networks, *Eur. Phys. J. B* **49**, 231 (2006).
- [31] Y. Baek, D. Kim, M. Ha, and H. Jeong, Fundamental structural constraint of random scale-free networks, *Phys. Rev. Lett.* **109**, 118701 (2012).
- [32] M. E. J. Newman, S. H. Strogatz, and D. J. Watts, Random graphs with arbitrary degree distributions and their applications, *Phys. Rev. E* **64**, 026118 (2001).
- [33] M. Molloy and B. Reed, A critical point for random graphs with a given degree sequence, *Random Struct. Algor.* **6**, 161 (1995).
- [34] M. E. J. Newman and G. T. Barkema, *Monte Carlo methods in statistical physics* (Oxford University Press, 1999).
- [35] W. Aiello, F. Chung, and L. Lu, A random graph model for power law graphs, *Exp. Math.* **10**, 53 (2001).
- [36] S. S. Manna and A. Chatterjee, A new route to explosive percolation, *Physica A* **390**, 177 (2011).
- [37] J. Fan, J. Meng, Y. Liu, A. A. Saberi, J. Kurths, and J. Nagler, Universal gap scaling in percolation, *Nat. Phys.* **16**, 455 (2020).
- [38] Q. Shi, S. Wei, Y. Deng, and M. Li, Universality of percolation at dynamic pseudocritical point, *Chinese Phys. B* **34**, 040501 (2025).
- [39] M. Li, J. Wang, and Y. Deng, Explosive percolation obeys standard finite-size scaling in an event-based ensemble, *Phys. Rev. Lett.* **130**, 147101 (2023).
- [40] M. Li, J. Wang, and Y. Deng, Explosive percolation in finite dimensions, *Phys. Rev. Research* **6**, 033319 (2024).
- [41] M. Molloy and B. Reed, The size of the giant component of a random graph with a given degree sequence, *Comb. Probab. Comput.* **7**, 295 (1998).
- [42] H. Bateman, *Higher Transcendental Functions*, edited by A. Erdélyi *et al*, Vol. I (McGraw-Hill Book Company, New York, 1953).
- [43] Z. Wu, C. Lagorio, L. A. Braunstein, R. Cohen, S. Havlin, and H. E. Stanley, Numerical evaluation of the upper critical dimension of percolation in scale-free networks, *Phys. Rev. E* **75**, 066110 (2007).
- [44] M. Li, S. Fang, J. Fan, and Y. Deng, Crossover finite-size scaling theory and its applications in percolation, *arXiv* , 2412.06228 (2024).
- [45] T. Kalisky and R. Cohen, Width of percolation transition in complex networks, *Phys. Rev. E* **73**, 035101 (2006).
- [46] M. Catanzaro, M. Boguñá, and R. Pastor-Satorras, Generation of uncorrelated random scale-free networks, *Phys. Rev. E* **71**, 027103 (2005).
- [47] A. V. Goltsev, S. N. Dorogovtsev, and J. F. F. Mendes, Percolation on correlated networks, *Phys. Rev. E* **78**, 051105 (2008).
- [48] S. Mizutaka and T. Hasegawa, Percolation on a maximally disassortative network, *Europhys. Lett.* **128**, 46003 (2020).
- [49] M. Lu, S. Fang, Z. Zhou, and Y. Deng, Interplay of the complete-graph and gaussian fixed-point asymptotics in finite-size scaling of percolation above the upper critical dimension, *Phys. Rev. E* **110**, 044140 (2024).
- [50] M. Lu, Y.-F. Song, M. Li, and Y. Deng, Self-similar gap dynamics in percolation and rigidity percolation, *arXiv* , 2411.04748 (2024).